Electronic Supplementary Material (ESI) for Dalton Transactions.

Supplementary information

Alkali hexatitanate photocatalysts with various morphologies for selective reduction of carbon dioxide by water

Xing Zhu,[a] Akira Yamamoto,[a,b] and Hisao Yoshida[a,b,*]

[a] *Graduate School of Human and Environmental Studies, Kyoto University, Kyoto 606-8501, Japan*

[b] *Elements Strategy Initiative for Catalysts and Batteries (ESICB), Kyoto University, Kyoto 615-8520, Japan*

**Corresponding author:* yoshida.hisao.2a@kyoto-u.ac.jp

1. Crystal structure and morphology of potassium hexatitanate

In the current study, fabrication of four kinds of alkali hexatitanate, sodium hexatitanate NTO(70%NaCl, 1273K), potassium hexatitanate KTO(70%NaCl, 1273K), rubidium hexatitanate RTO(70%NaCl, 1273K) and cesium hexatitanate CTO(70%NaCl, 1273 K) were examined by a flux method with a NaCl flux. However, except the KTO(70%NaCl, 1273K) sample, the diffraction lines of other three samples were resemble to those of the $Na_2Ti_6O_{13}$ reference (Figure S1). This indicated that the NaCl flux could react with these raw materials easily.

The SEM images showed that the prepared four samples consisted of similar roundish rod-like particles (Figure S2a, b c and d), while the particles of KTO(70%NaCl, 1273K) sample were more uniform and fine particles (Figure S2b).

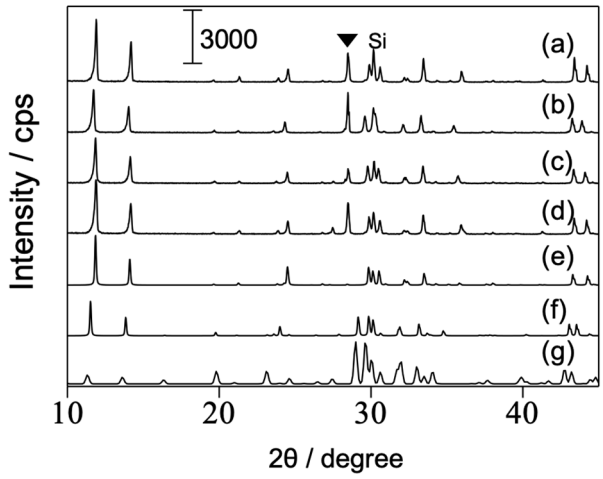

Figure S1. XRD patterns of the prepared $A_2Ti_6O_{13}$ samples with a 70% NaCl flux, (a) NTO(70%NaCl, 1273K), (b) KTO(70%NaCl, 1273K), (c) RTO(70%NaCl, 1273K), and (d) CTO(70%NaCl, 1273K). Samples were heated at 1273 K for 10 h. The references from the ICSD database are also shown, (e) ICSD#23877 for $Na_2Ti_6O_{13}$, (f) ICSD#25712 for $K_2Ti_6O_{13}$, and (g) ICSD#23878 for $Rb_2Ti_6O_{13}$. Closed triangles indicate silicon powder mixed with the samples to calibrate the diffraction angle.

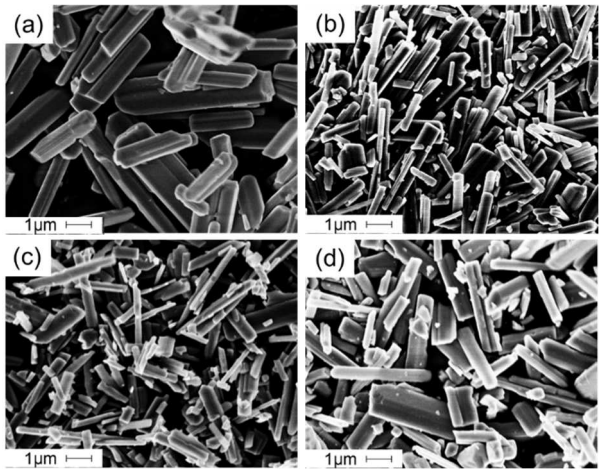

Figure S2. SEM images of the prepared $A_2Ti_6O_{13}$ samples heated at 1273 K for 10 h by the flux method with a 70% NaCl flux. (a) NTO(70%NaCl, 1273K), (b) KTO(70%NaCl, 1273K), (c) RTO(70%NaCl, 1273K), and (d) CTO(70%NaCl, 1273K).

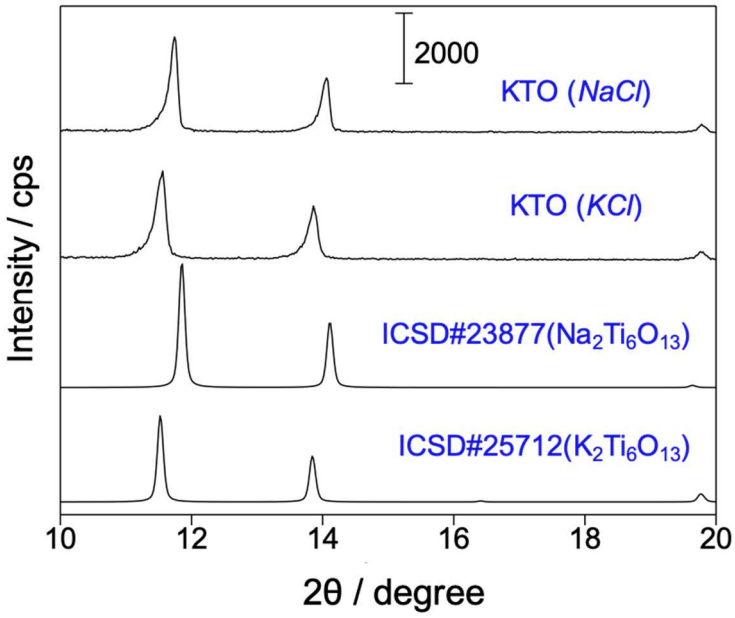

Figure S3. XRD patterns of the $K_2Ti_6O_{13}$ samples prepared with different fluxes and some references.

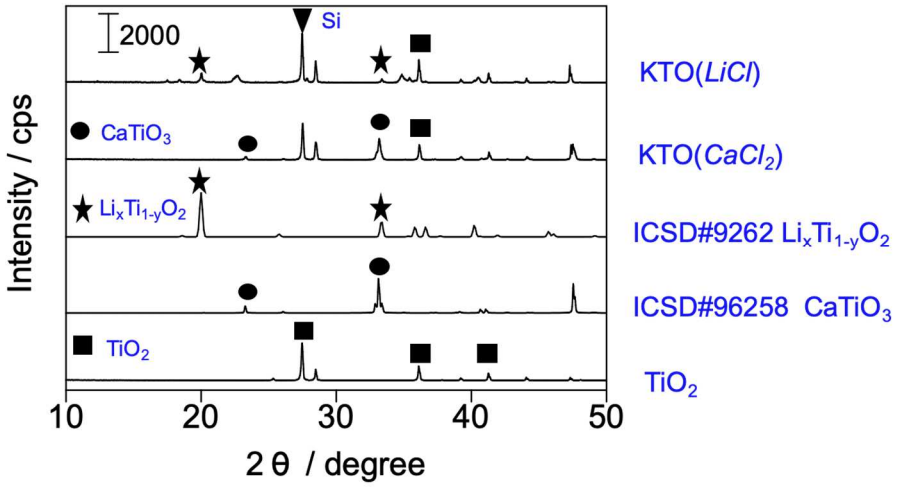

Figure S4. XRD patterns of the $K_2Ti_6O_{13}$ samples prepared with different fluxes and some references.

XRD patterns of the prepared samples (Figure S5) show that the pristine KTO samples were successfully fabricated in this study, since no impurity was observed. And some differences in diffraction lines were also found. For example, although the intensity of line at 11.52° corresponding to (200) plane of the KTO(10%KCl, 1373K) sample is quite close to that of the KTO(SSR, 1373K) sample, with the increasing amount of involved KCl flux, this intensity increased gradually, implying that the KCl flux was beneficial to the growth of the facet corresponded to (200) plane for KTO crystals. And this resulted in an anisotropic morphology for the prepared KTO sample.

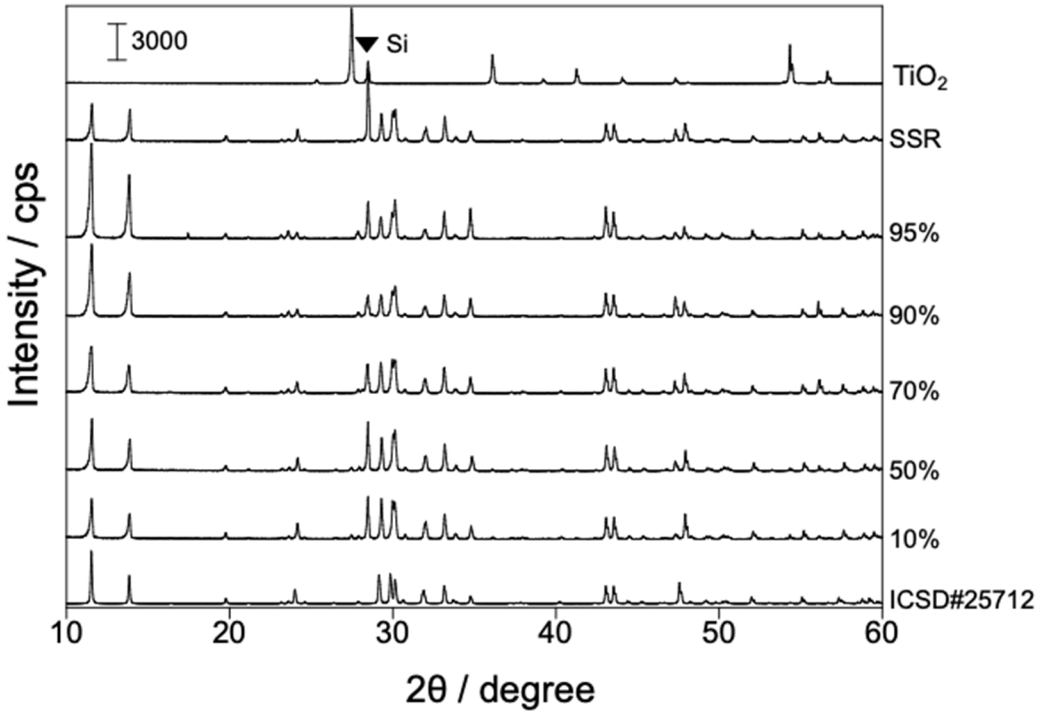

Figure S5. XRD patterns of the KTO(*x*%KCl, 1373K) samples prepared with different ratio of the KCl flux.

Table S1. The average sizes of the rod-like crystals in the KTO (70%KCl, *y*K) samples heated at different temperature.

Heating temperature (K)	Width (μm)	Length (μm)
1073	0.09	0.45
1173	0.19	0.82
1273	0.25	1.25
1373	0.45	2.00
1473	0.73	2.33
1573	1.37	3.32

As were shown in Figures S6 and S7, it was found 10 h is the most proper heating time for the crystals to grow since no TiO_2 was observed. While some impurity spectra corresponded to the TiO_2 were observed for other samples (Figure S7). The SEM images in Figure S8 showed that the very similar rod-like particles were fabricated, but the KTO sample heated for 10 h consisted of quite uniform particles, and this may be one of the reasons for its highest photocatalytic activity for CO_2 reduction by H_2O shown in Figure S9.

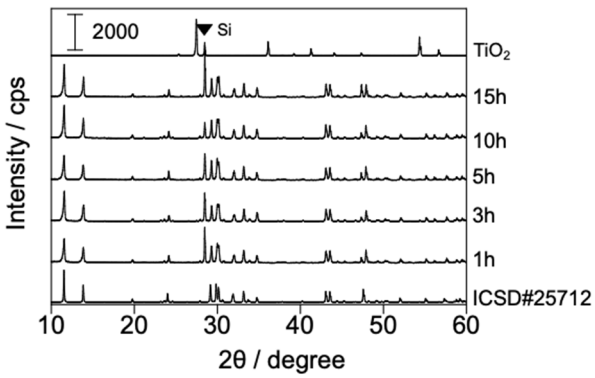

Figure S6. XRD patterns of the KTO(70%KCl, 1273K) samples prepared by a flux method at different holding time.

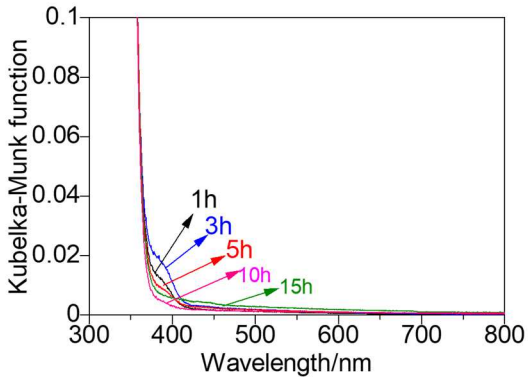

Figure S7. DR UV-vis spectra of the KTO(70%KCl, 1273K) samples prepared by a flux method at different holding time.

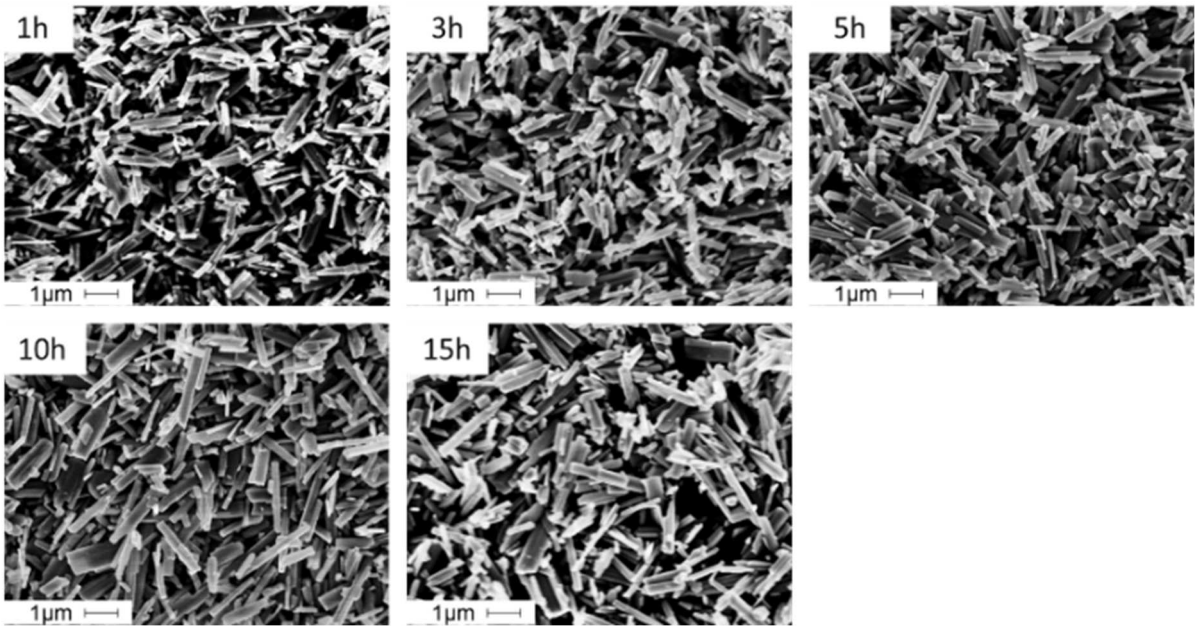

Figure S8. SEM images of the KTO(70%KCl, 1273K) samples prepared by a flux method at different holding time.

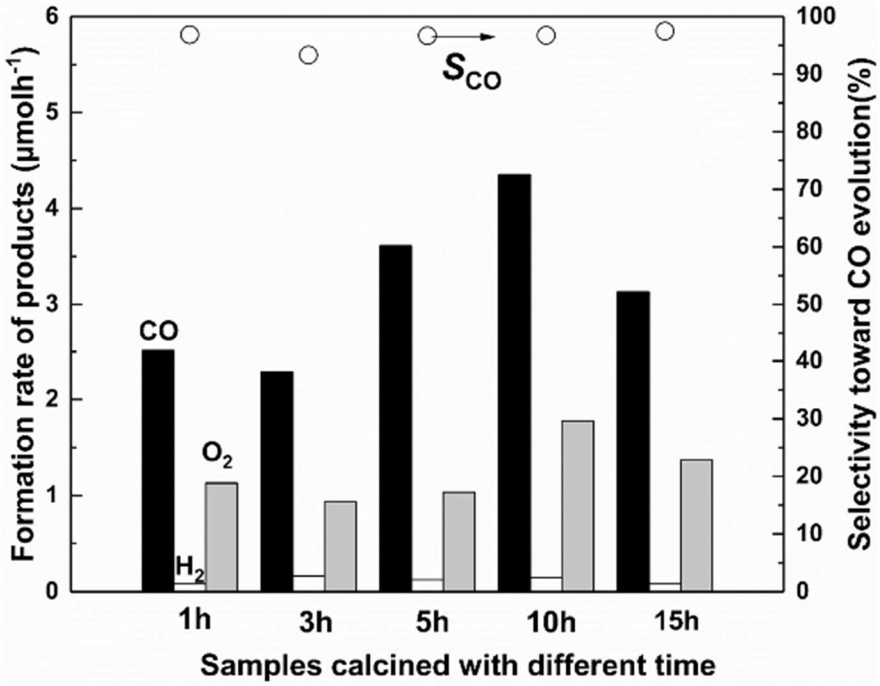

Figure S9. photocatalytic activity of CO (black bar), H_2 (white bar), O_2 (grey bar) and the S_{CO} evolution (open circles) over the KTO(70%KCl, 1273K) samples prepared by a flux method at different holding time.

The cooling rate was reported to affect the growth of crystal as well in our previous studies,[S1,S2] and it was suggested as follows: the solutes, K_2CO_3 and TiO_2, should be dissolved in enough amount of molten salt, and then the crystallization of $K_2Ti_6O_{13}$ would take place during the cooling step due to the decreasing solubility of the solutes in the flux. It is expected that this dissolution-crystallization process would provide the hexagonal rod-like crystal naturally with fewer defects and fewer crystallites boundaries. As were shown in Figure S10 and S11, when the cooling rate varied from −25 K h^{-1} to −200 K h^{-1}, the morphologies of prepared samples were not obviously different from each other, and the sample prepared by a flux method with the cooling rate of −100 K h^{-1} exhibited the highest activity. It is difficult to explain the reason exactly.

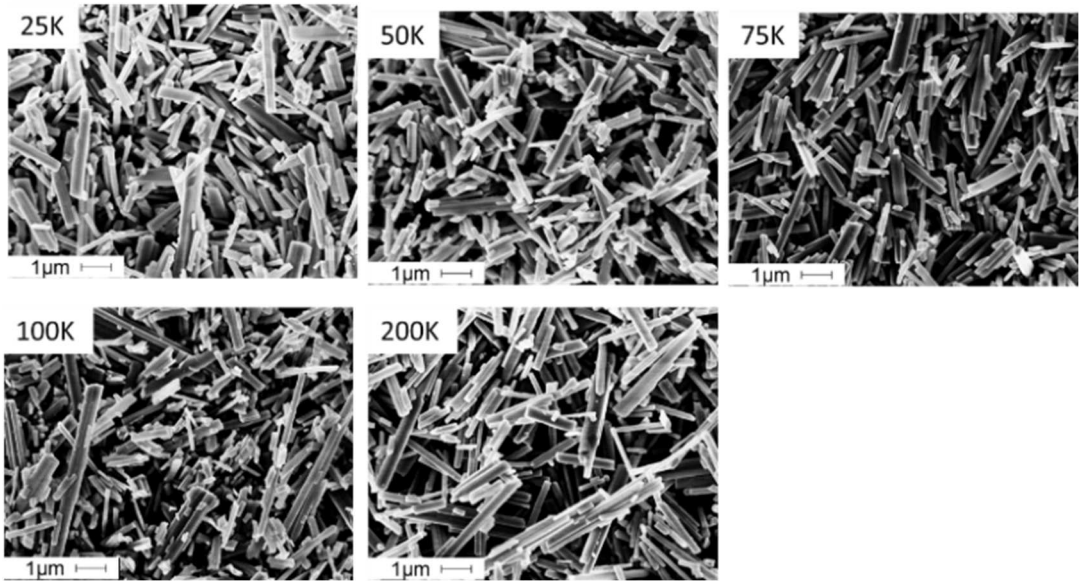

Figure S10. SEM images of the KTO(70%KCl, 1273K) samples prepared by a flux method at different cooling rate per hour.

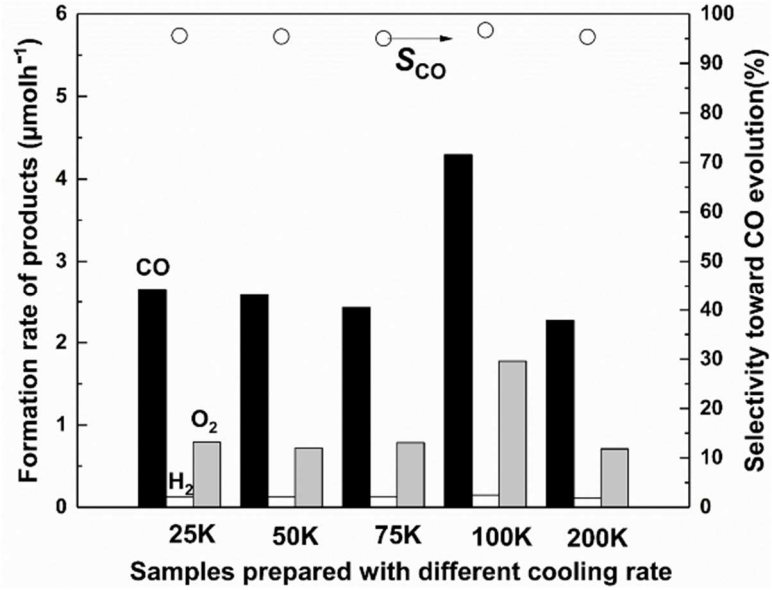

Figure S11. Photocatalytic activity of CO (black bar), H_2 (white bar), O_2 (grey bar) and the S_{CO} evolution (open circles) over the KTO(70%KCl, 1273K) samples prepared by a flux method at different cooling rate per hour.

2. Ag cocatalyst

A comparison experiments were conducted here to figure out the influence of differently prepared $K_2Ti_6O_{13}$ crystals as the support for Ag cocatalyst. It was found that Ag cocatalysts were loaded on the long facets with very similar particle sizes in the Ag/KTO(70%KCl, 1273K) and Ag/KTO(70%KCl, 1373K) samples. Neither for loaded facets nor particle size of Ag cocatalyst, there was and no obvious difference between these two samples.

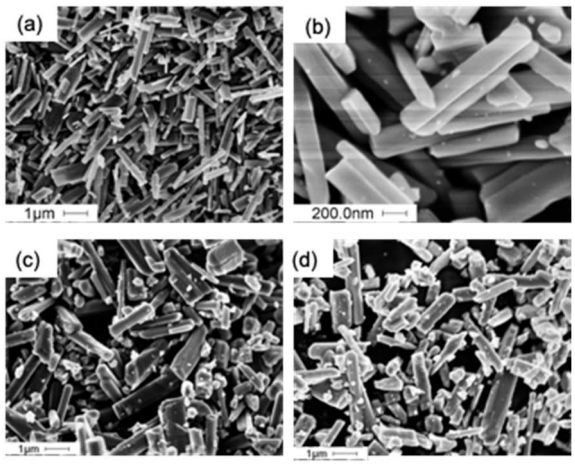

Figure S12. SEM images of the prepared samples, (a) KTO(70%KCl, 1273K), (b) Ag/KTO(70%KCl, 1273K), (c) KTO(70%KCl, 1373K), and (d) Ag/KTO(70%KCl, 1373K).

3. Correlation between photocatalytic activity, aspect ratio

Table S2. Results of the reaction tests for the photocatalytic reduction of CO_2 with H_2O with the 1 wt% Ag/KTO samples, and crystallite size along the plane, and aspect ratio along two planes of KTO(*x*%KCl, 1373K) samples prepared with different ratio of flux.

Samples	Formation rater (μmol h^{-1})			Crystallite size along the plane			Aspect ratio along two planes		
	CO	H_2	O_2	201	020	200	201/200	020/201	020/200
SSR	2.50	0.34	0.38	91.6	179.3	87.9	1.04	1.96	2.04
10%	3.63	0.63	0.77	106.4	259.8	115.8	0.92	2.44	2.24
50%	3.98	0.90	0.46	49.5	104.5	47.1	1.05	2.11	2.22
70%	4.48	0.18	0.94	52.0	162.9	52.0	0.98	3.20	3.13
90%	2.15	0.14	0.49	61.9	166.1	60.9	1.02	2.68	2.73
95%	2.35	0.51	0.69	287.7	380.7	126.2	1.32	1.3	3.02

Table S3. Results of the reaction tests for the photocatalytic reduction of CO_2 with H_2O with the 1 wt% Ag/KTO samples, and crystallite size along the plane and aspect ratio along two planes of KTO(70%KCl, yK) samples prepared with different heating temperature.

Samples	Formation rater (μmol h^{-1})			Crystallite size along the plane			Aspect ratio along two planes		
	CO	H_2	O_2	201	020	200	201/200	020/201	020/200
1073K	1.85	0.15	0.44	38.0	85.0	40.7	0.93	2.24	2.09
1173K	2.38	0.13	0.79	49.6	164.5	56.3	0.88	3.32	2.92
1273K	4.35	0.15	1.78	39.9	108.5	38.1	1.05	2.72	2.85
1373K	4.48	0.18	0.94	49.5	104.0	47.2	1.05	2.11	2.22
1473K	1.19	0.20	0.48	72.8	259.8	73.1	1.00	3.57	3.56
1573K	0.65	0.26	0.42	100.0	185.1	109.3	0.93	2.24	2.09

As were shown in Figure S13a and b, when the aspect ratio of 020/200 and 020/201 was around 2.1 and 2.2, respectively, the CO evolution was the maximum among these results with the samples prepared in different ratio of the flux. On the other hand, the optimized ratios were around 2.8 and 2.6 among the samples prepared at different temperatures. Additionally, the aspect ratio along two 020/200 planes was increased when the flux ratio was increased. When the holding temperature increased, crystallite size became larger as shown in Table S3.

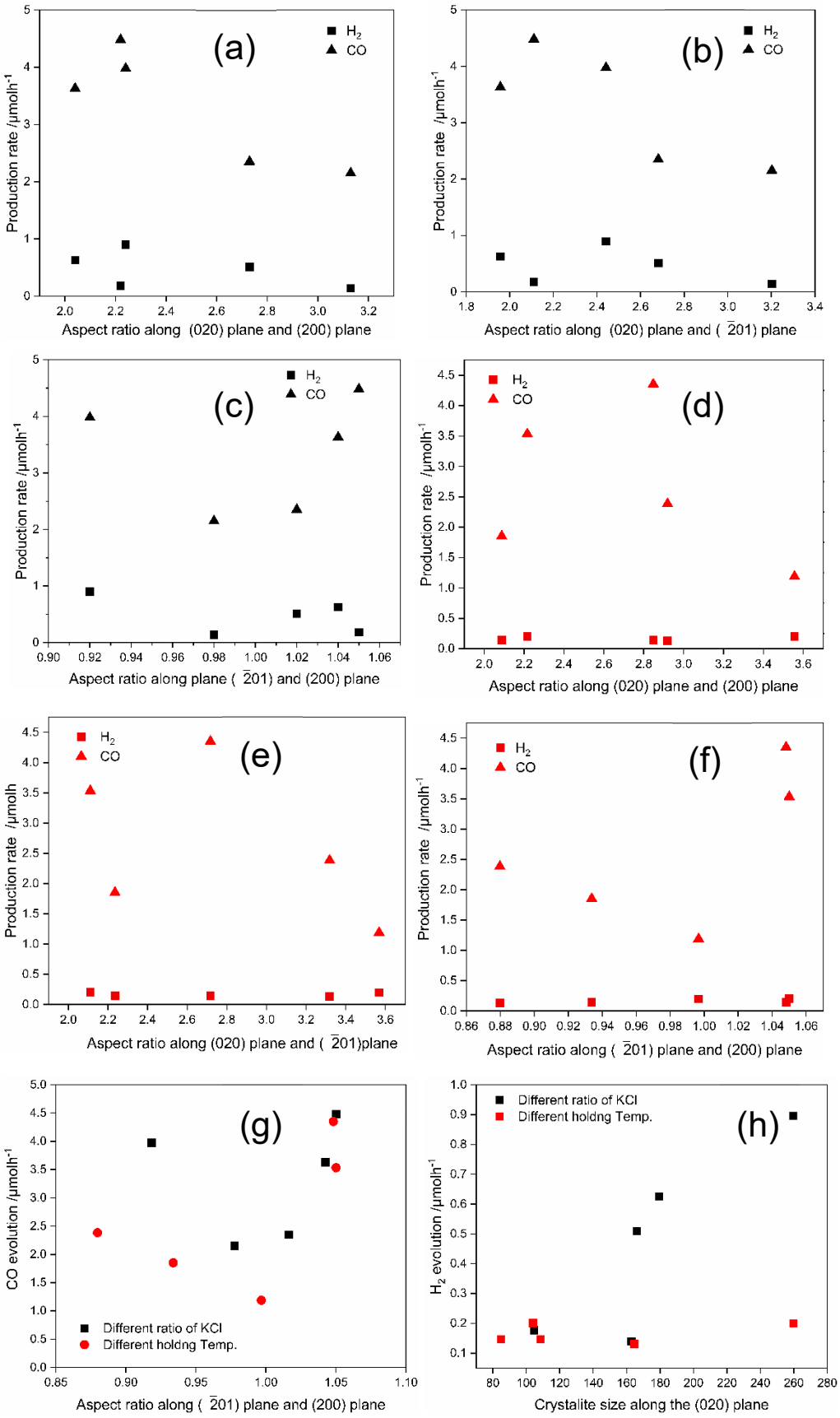

Figure S13. Correlation between formation rate of CO and H_2 and aspect ratio, or crystallize size of some facets, (a)-(c) samples prepared with different ratio of KCl flux, (d)-(f) samples prepared at different holding temperature, (g) summary of these two groups, (h) the correlation between crystallite size along the 020 plane and H_2 evolution.

4. Stability and durability of the prepared sample

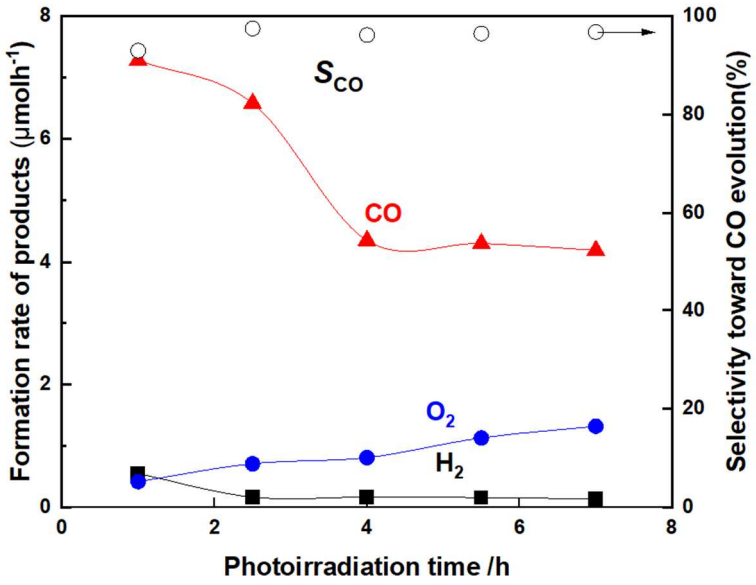

Fig. S14 The second cycle of the time course of the photocatalytic formation rate of the products and the R(e^-/h^+) value over the Ag/KTO(70%KCl, 1273K) sample, which was prepared under the optimized conditions by the flux method, followed by loading 1 wt% Ag cocatalyst by a PD method.

5. Comparison with reported photocatalysts

Table S4 Comparison of the photocatalytic activity of the reported Ag-loaded photocatalysts in our laboratory.

Photocatalyst	Weight of sample (g)	Volume of water (L)	High pressure mercury Lamp (W)	CO evolution activity (μmol h^{-1})	CO selectivity (%)	Ref.
Ag /$K_2Ti_6O_{13}$	0.2	0.35	100	4.3	96	Current study
Ag/$Na_2Ti_6O_{13}$	0.3	0.35	100	2.8	82	S3
Ag/$CaTiO_3$	0.3	0.35	100	7.3	96	S4
Ag/$CaZrO_3$	0.5	1.0	400	1.8	41	S5

Rreferences

S1 H. Yoshida, M. Sato, N. Fukuo, L. Zhang, T. Yoshida, Y. Yamamoto, T. Morikawa, T. Kajino, M. Sakano, T. Sekito, S. Matsumoto and H. Hirata, *Catal. Today*, 2018, **303**, 296–304.

S2 H. Yoshida, L. Zhang, M. Sato, T. Morikawa, T. Kajino, T. Sekito, S. Matsumoto and H. Hirata, *Catal. Today*, 2015, **251**, 132–139.

S3 X. Zhu, A. Anzai, A. Yamamoto and H. Yoshida, *Appl. Catal. B Environ.*, 2019, **243**, 47–56.

S4 T. Soltani, X. Zhu, A. Yamamoto, S. P. Singh, E. Fudo, A. Tanaka, H. Kominami and H. Yoshida, *Appl. Catal. B Environ.*, 2021, **286**, 119899.

S5 T. Ishii, A. Anzai, A. Yamamoto and H. Yoshida, *Appl. Catal. B Environ.*, 2020, **277**, 119192.